ARMY RESEARCH LABORATORY

Quantifying Damage at Multiple Loading Rates to Kevlar KM2 Fibers Due to Weaving and Finishing

by Brett D. Sanborn and Tusit Weerasooriya

ARL-TR-6465 **June 2013**

NOTICES

Disclaimers

The findings in this report are not to be construed as an official Department of the Army position unless so designated by other authorized documents.

Citation of manufacturer's or trade names does not constitute an official endorsement or approval of the use thereof.

Destroy this report when it is no longer needed. Do not return it to the originator.

Army Research Laboratory
Aberdeen Proving Ground, MD 21005-5069

ARL-TR-6465 **June 2013**

Quantifying Damage at Multiple Loading Rates to Kevlar KM2 Fibers Due to Weaving and Finishing

Brett D. Sanborn
Oak Ridge Institute for Science and Education

Tusit Weerasooriya
Weapons and Materials Research Directorate, ARL

REPORT DOCUMENTATION PAGE

Form Approved
OMB No. 0704-0188

1. REPORT DATE *(DD-MM-YYYY)*	**2. REPORT TYPE**	**3. DATES COVERED (From - To)**
June 2013	Final	February 2012–February 2013

4. TITLE AND SUBTITLE

Quantifying Damage at Multiple Loading Rates to Kevlar KM2 Fibers Due to Weaving and Finishing

5a. CONTRACT NUMBER

5b. GRANT NUMBER

5c. PROGRAM ELEMENT NUMBER

6. AUTHOR(S)

Brett D. Sanborn* and Tusit Weerasooriya

5d. PROJECT NUMBER

5e. TASK NUMBER

5f. WORK UNIT NUMBER

7. PERFORMING ORGANIZATION NAME(S) AND ADDRESS(ES)

U.S. Army Research Laboratory
ATTN: RDRL-WMP-B
Aberdeen Proving Ground, MD 21005-5069

8. PERFORMING ORGANIZATION REPORT NUMBER

ARL-TR-6465

9. SPONSORING/MONITORING AGENCY NAME(S) AND ADDRESS(ES)

10. SPONSOR/MONITOR'S ACRONYM(S)

11. SPONSOR/MONITOR'S REPORT NUMBER(S)

12. DISTRIBUTION/AVAILABILITY STATEMENT

Approved for public release; distribution is unlimited.

13. SUPPLEMENTARY NOTES

*Oak Ridge Institute for Science and Education, 4692 Millennium Dr., Ste. 101, Belcamp, MD 21017

14. ABSTRACT

Numerical simulation of impact events on fabric-based protective systems requires accurate mechanical characterization of the constituent material at similar strain rates as the impact event. Because Kevlar (Kevlar is a registered trademark of DuPont Company) yarn is woven into fabric to make protective equipment, the strength of the individual filaments may become compromised as a result of the crimping, weaving process, or finishing process. To elucidate and quantify any damage to the fibers as a result of the weaving or post treatment finishing process, single fibers were extracted from the warp and weft directions of plain woven, hydrophobically treated Kevlar cloth and the strength was measured over a wide range of strain rates and compared to the response of fibers extracted from an unwoven yarn. The tensile strength of fibers from the warp, weft, and unwoven Kevlar were evaluated at 0.001 s^{-1}, 1 s^{-1}, and approximately 1000 s^{-1} using a Bose Electroforce test setup and a Hopkinson tension bar modified for fiber experiments. A wide range of gage lengths from 2 to 150 mm was investigated to find the effect of defect distribution on the tensile strength of the single fibers. The results show that fibers taken from the weft direction of the woven fabric decreased in strength 3%–8% compared to the unwoven fiber. The warp fibers were a minimum of 20% weaker than unwoven and weft fibers at all loading rates. Measured Young's Modulus as a function of strain rate and tensile strength as a function of gage length are also presented in this technical report.

15. SUBJECT TERMS

SHTB, Kevlar KM2, single fiber, tensile strength degradation, high rate, stress-strain, loading rate, weaving, plain woven

16. SECURITY CLASSIFICATION OF:			**17. LIMITATION OF ABSTRACT**	**18. NUMBER OF PAGES**	**19a. NAME OF RESPONSIBLE PERSON**
a. REPORT	**b. ABSTRACT**	**c. THIS PAGE**			Brett D. Sanborn
Unclassified	Unclassified	Unclassified	UU	34	**19b. TELEPHONE NUMBER** (*Include area code*) 410-306-4925

Standard Form 298 (Rev. 8/98)
Prescribed by ANSI Std. Z39.18

Contents

List of Figures

List of Tables

Acknowledgments

Thanks to Nicole Racine and Andrew Hoosier for their help making fiber samples and performing tests. Thanks to Tishan Weerasooriya for his help in measuring fibers.

1. Introduction

Kevlar* fiber has highly oriented polymer chains produced from poly-paraphenylene (PPTA). Because Kevlar is much stronger in the axial direction than the transverse direction, and due to its high strength and light weight, Kevlar has seen wide use in flexible armor applications. Obtaining mechanical properties of single fibers at multiple strain rates is important for simulation of impact on fiber-based protective systems, which will ultimately be used for improved design of such protective systems. Accurate simulation of flexible fiber-based armor requires material models derived from accurate material properties collected under valid experimental conditions. The behavior of the fiber material may be different depending on the processing methods. Specifically in the case of Kevlar fabric, the weaving method used to form the raw Kevlar yarns into woven fabric affects the strength of the fibers, and therefore must be investigated to quantify the damage due to processing.

Through different methods of fiber processing and weaving, the strength of the individual filaments in a yarn of Kevlar may become altered. High-performance fibers are woven into a variety of weave styles depending on the application including crowfoot, plain leno, basket, and plain woven (*1*). This study only looks at Kevlar KM2 fiber that has been plain woven and treated with a hydrophobic finish. Plain weaving consists of yarns in the warp direction held in tension, while the weft (or fill) yarns are inserted between alternating warp yarns, as shown in figure 1. During this weaving process, it is feasible that the strength of the individual filaments in the yarns become compromised. This possible reduction in strength could be due to the crimping of the yarns, the pretension applied to the warp fibers, frictional interaction between the fibers during weaving, friction interaction between yarns and weaving equipment, or post treatment processing, such as the application of a hydrophobic fluoropolymer. Any difference in strength between the warp and the weft fibers compared to the unwoven fibers will affect the results from computational efforts aimed at simulating impact on the fiber-based protective system; realistic and accurate values for the ultimate strength of fibers taken from each direction must be used in such computer codes. Quantification of any damage in the warp and weft fibers will also provide insights that may help develop methods to reduce damage of the fibers during processing.

*Kevlar is a registered trademark of DuPont Company.

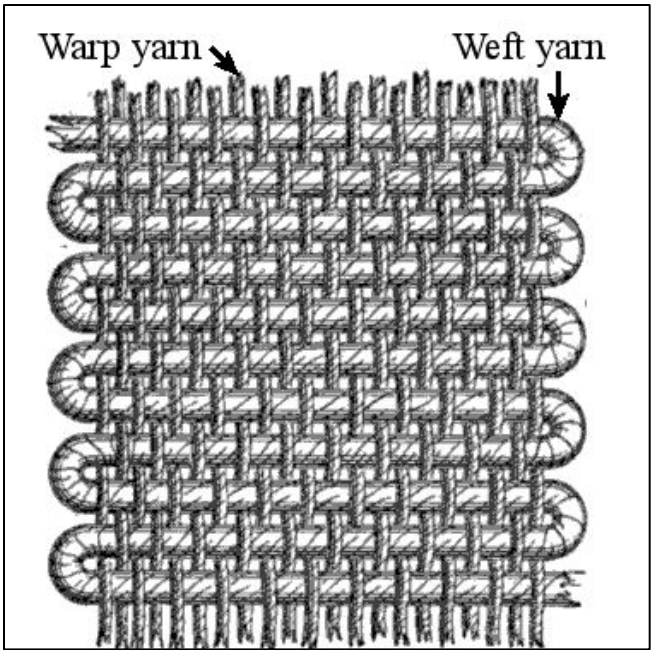

Figure 1. Layout of warp and weft yarns in a plain woven fabric.

Experimental methods to record the mechanical response of single fibers, and specifically Kevlar, have existed since at least the early 1980s (*2*). However, methods to study the high-rate response of single fibers have been created only in the last decade (*3*). Cheng et al. (*3*) conducted the first investigation of single fiber response at loading rates up to approximately 2500 s^{-1}. Using a modified split-Hopkinson tension bar (fiber-SHTB), Cheng et al. (*3*) found that at high-loading rates, the stress-strain response of the approximately 12-µm-diameter Kevlar fiber was linear and elastic until failure. Additionally, Cheng et al. (*3*) found that the strength of Kevlar was weakly loading-rate dependent; only a small increase in failure strength was noted when the loading rate was increased from quasi-static (0.00127 s^{-1}) to high rate (2500 s^{-1}). At quasi-static strain rates, Cheng et al. (*3*) found that the strength of the unwoven Kevlar KM2 was 3.88 ± 0.40 GPa, while at high rate the strength of the fiber was 4.04 ± 0.38 GPa. Cheng et al. (*4*) also developed an experimental technique to characterize the transverse mechanical behavior of fibers. Using this new technique, Cheng et al. (*4*) showed that the fiber was transversely isotropic, and the transverse modulus was 1 order of magnitude lower than the longitudinal modulus.

Using similar methods as Cheng et al. (*3*), Lim et al. (*5*) studied the rate dependent behavior of A265 single fibers. Lim et al. (*5*) looked at gage length dependent defects in the A265 fibers. In another publication, Lim et al. (*6*) improved the experimental setup presented by Cheng et al. (*3*) by introducing a laser extensometer method to accurately measure the small displacement behavior of the bar end and subsequently to measure the strain of the fiber. Lim et al. (*6*) also employed the correction for compliance in the fiber testing system given in ASTM 1557-03 (*7*)

to both the quasi-static and high-rate results. Lim et al. (*8*) investigated rate effects and gage length effects in Kevlar fiber taken from protective vests over a 10-year range. The type of Kevlar in the vests was not specified in that study. In addition, in the publication, comparisons of the strength of the warp and weft fibers were not made to the strength of unwoven fibers of the same fiber type and denier, nor were the finishing process of the woven fabric mentioned. Hence, it is necessary to study the effect of weaving on Kevlar single fibers at all loading rates, especially relative to the unwoven fibers.

Nilakantan et al. (*9*) completed an experimental evaluation of strength and strain energy density for failure on Kevlar KM2 yarns, exploring both length-scale and weaving effects. The experiments were completed on Kevlar KM2 600 denier unwoven yarn and compared to yarns taken from the warp and weft directions of KM2 style 706 woven fabrics. The finishes applied to the style 706 fabrics were greige (unfinished, loom state fabric) and scoured, which includes chemical treatment and washing with proprietary additives after the weaving process is finished. Strength of the warp and weft yarns degraded compared to the unwoven yarn. The warp yarns were found to be 16% weaker than unwoven in the greige case and 30% weaker than the unwoven yarns in the scoured case. The weft fibers were 8% and 11% weaker for the greige and scoured cases, respectively.

The study reported in this paper is an expansion of a previous investigation of weaving effects by Sanborn et al. (*10*). The previous study was limited to specimens of one gage length. Consequently, the dependence of gage length and subsequently defect distribution on failure strength could not be concluded from that study. In this study, the strength of fibers extracted from the warp and weft directions of Kevlar KM2 style 706 (plain woven, CS-898 hydrophobic finish), 600 denier fabric are compared to the strength of previously unwoven fibers taken from 600d yarn allowing to quantify damage to the single fibers due to the plain weaving process. Specimens of gage lengths of 2, 5, 10, 50, 100, and 150 mm were studied to measure the effect of the defect distribution in the unwoven, warp, and weft Kevlar KM2 single fibers. The strain rate is increased from quasi-static (0.001 s^{-1}), to intermediate (1 s^{-1}), and finally to high rate (approximately 1000 s^{-1}) to investigate strain rate effects in the unwoven and woven fibers. Comparisons of strength of the unwoven and woven fibers will help to reveal any reduction in strength at multiple loading rates.

2. Experiments

2.1 Materials

To study the effect of plain weaving on the strength of individual Kevlar fibers, never woven (virgin fibers) were extracted from a spool of Kevlar KM2 600 denier yarn. Warp and weft

samples were taken from style 706 Kevlar fabric, because style 706 is composed of 600d yarn. The fabric is pulled several times through a series of rollers submerged in a mixture of hot, soapy water to cleanse the surface. This high-speed, possibly violent process may alter the properties of the woven fabric. The 706 fabric was coated with a water repellant finish (CS-898) following the scouring or washing process. After being coated with the fluropolymer, the fabric is subjected to an elevated temperature to cure the fluoropolymer coating. Unfortunately, the information relating to the scouring and hydrophobic treating processes are proprietary, so the specific data such as exact temperatures during processing is not available.

To study the rate dependency of the mechanical response, experiments were conducted at quasi-static, intermediate, and high rate that correspond to strain rates of 0.001 s^{-1}, 1 s^{-1}, and approximately 1000 s^{-1}, respectively. High-rate experiments were conducted using a SHTB that was modified for fiber characterization while low and intermediate rate behavior was captured using a Bose Electroforce experimental setup.

An investigation of the effect of varying the gage length was also completed to elucidate any distribution of defects along the fiber. For each of the three types of fibers (warp, weft, and unwoven), quasi-static and intermediate rate experiments were conducted at gage lengths including 2, 5, 10, 50, 100, and 150 mm. Gage lengths for high-rate experiments were limited to 2, 5, and 10 mm, because dynamic equilibrium of the fiber sample is difficult to achieve for longer gage lengths. At each condition of strain rate and gage length 10 experiments were conducted. The complete experimental test matrix is shown in table 1.

Table 1. Experimental test matrix. Ten experiments at each condition were conducted.

Gage Length (mm)	Low Rate 0.001/s			Intermediate Rate 1/s			High Rate 1200/s		
	Unwoven	Warp	Weft	Unwoven	Warp	Weft	Unwoven	Warp	Weft
2	10	10	10	10	10	10	10	10	10
5	10	10	10	10	10	10	10	10	10
10	10	10	10	10	10	10	10	10	10
50	10	10	10	10	10	10			
100	10	10	10	10	10	10		Total:	450
150	10	10	10	10	10	10			

Fibers were affixed to cardboard specimen holders using 3M Scotch-Weld* Structural Plastic Adhesive (DP-8005). Various geometries of specimen holders were used depending on the gage length and strain rate. The extracted fibers were glued to the cardboard specimen holders. Samples glued on the cardboard specimen holders were inserted into grips on the Bose Electroforce test setup. The sides of the specimen holder are clipped away allowing the fiber to span between the load cell and movable actuator. For high-rate specimens, slotted setscrews are glued on either side of the sample using cyanoacrylate glue. The sample is threaded into both the

* 3M and Scotch-Weld are trademarks of 3M Company.

bar end and load cell. Similar to the low and intermediate rate experiments, the sides of the specimen holder are removed allowing the fiber to span between the load cell and Hopkinson bar end, just before the specimen loading is initiated.

In an attempt to accurately obtain the stresses in each individual fiber, the diameter of each fiber sample was measured using a scanning electron microscope (SEM). Several samples were made from a single strand of fiber about 30 cm in length. After the fiber was secured by glue to the cardboard, a short piece (approximately 3 cm) of each fiber was cut from the end of the long strand and the diameter measurements were taken by imaging in the SEM. The diameter of the fiber was found to vary from 10.5 to 14 μm between strand to strand. A single average diameter value cannot be used for all fibers due to the variations that occur during production. Differences in the sizes of the holes in the spinnerette through which the raw PPTA polymer is extruded could be the reason for these variations, or perhaps each fiber may not experience the same amount of tension while being pulled from the spinnerette head into the water bath, and thus may not contract to the same diameter.

2.2 Quasi-Static and Intermediate Rate Experiments

The Bose Electroforce setup was used to evaluate the strength of the fiber at low and intermediate strain rates. The strain (ε) and strain rate ($\dot{\varepsilon}$) were calculated based on the gage length (l_s) of the sample:

$$\varepsilon = -\frac{d}{l_s} , \tag{1}$$

$$\dot{\varepsilon} = -\frac{v}{l_s} , \tag{2}$$

where d is the diameter of the specimen measured using the SEM, and v is the velocity of the experiment. The specimen stress is calculated using

$$\sigma = \frac{P}{A_0} , \tag{3}$$

where A_o is the initial cross-sectional area, and P is the force measured by the load cell.

2.3 High-Rate Experiments

A fiber-SHTB was used to study the behavior of the fiber at elevated loading rates. A picture of the fiber-SHTB is shown in figure 2, and a schematic is shown in figure 3. The fiber-SHTB is similar to the bar described by Cheng et al. (*3*). The 1/4-in-diameter aluminum incident bar has a flange threaded onto one end. Compressed air is used to fire the tubular striker bar at the impact flange. A tensile pulse is generated that travels down the incident bar and pulls the fiber specimen in tension at an approximate strain rate of 1000 s^{-1}. Part of the incident stress pulse is transmitted through the specimen while part is reflected back in the bar as a compression pulse.

Since the fibers are extremely weak, with typical measured loads are on the order of 0.5 N, a traditional transmission bar cannot be used to capture the transmitted signal. Instead, a fast-acting piezoelectric quartz load cell is used to collect the force history.

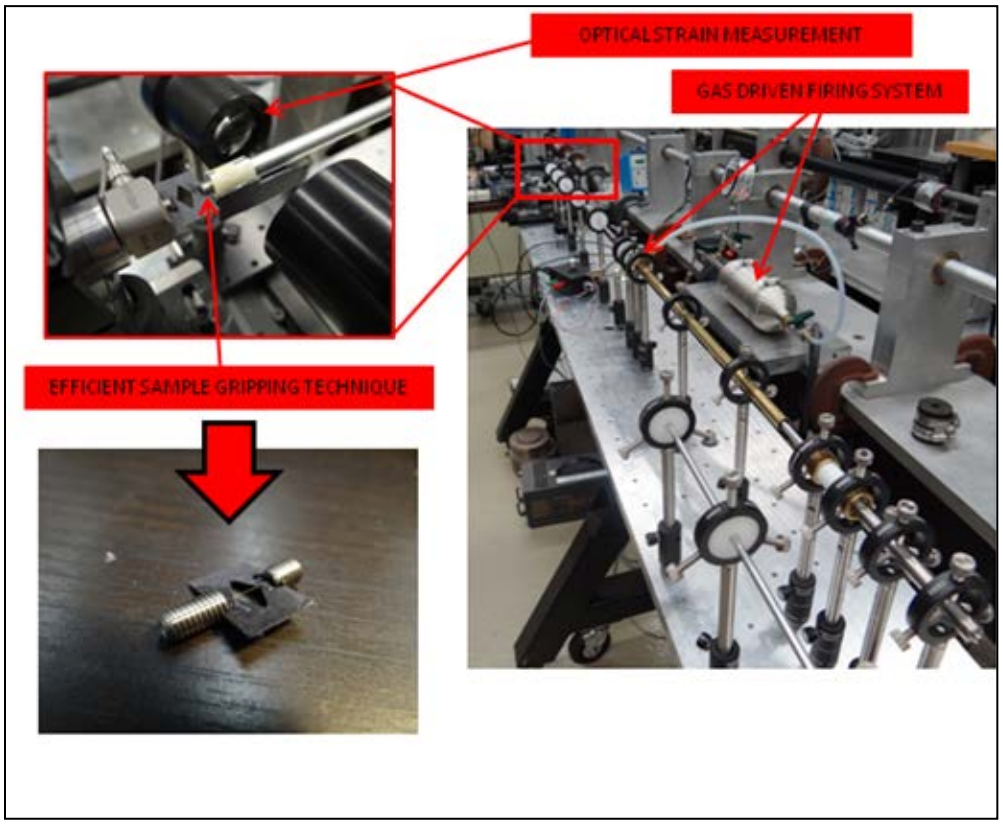

Figure 2. Modified fiber-SHTB and the fiber specimen for high-rate mechanical characterization of fibers.

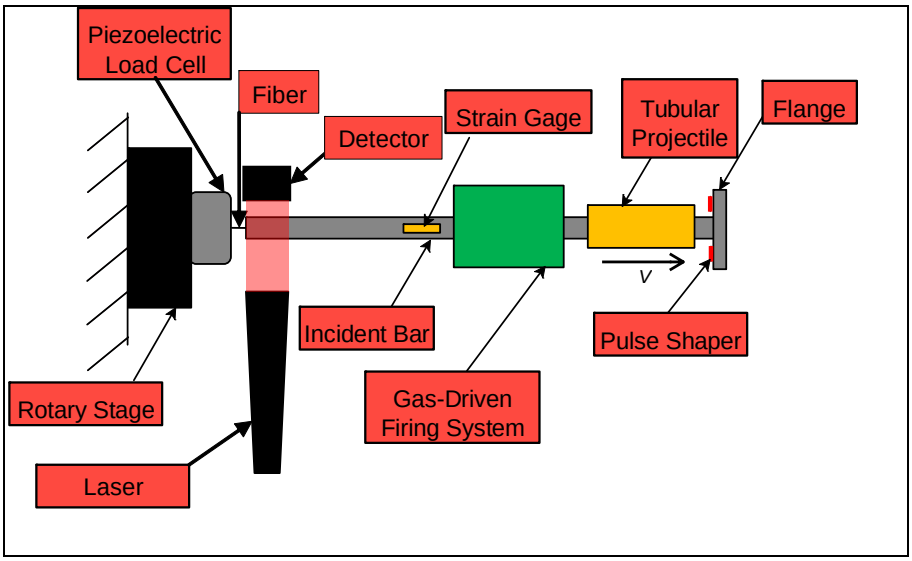

Figure 3. Schematic of fiber-SHTB.

Similar to the quasi-static experiments, the strain rate of the specimen is calculated using equation 2, except in a different form because the velocity from the fiber-SHTB experiment is calculated based on the histories of the incident and reflected pulses:

$$\dot{\varepsilon} = -\frac{c_o}{l_s}(\varepsilon_i - \varepsilon_r)\ , \tag{4}$$

and the strain was calculated as

$$\varepsilon = -\frac{c_o}{l_s}\int_0^t(\varepsilon_i - \varepsilon_r)dt\ , \tag{5}$$

where c_o is the wave speed, and ε_i and ε_r are the incident and reflected pulses, respectively.

In addition to calculating the strain of the specimen using the strain gage signal, a noncontact high-rate laser method was used to measure the strain history of the specimen, similar to the one described by Lim et al. (5). This laser method uses a laser with a built-in lens that generates a uniformly intense 25.4-mm-wide plate of laser light. A high-speed laser detector located on the opposite side of the incident bar end sends the signal to the oscilloscope. The measurement is made by converting the motion of the end of the incident bar to a voltage output that is proportional to displacement. A calibration is made prior to experimentation using a micrometer to uncover the laser detector at known length-steps and recording the corresponding output voltage from the detector. Using this calibration curve, the laser movement can be converted to extension of the fiber, and hence equation 1 can also be used to calculate strain. The distance and strain measurements obtained using the strain gages on the bar and the laser method were found to agree with each other, as long as the strain gage factor was carefully calibrated for each set of experiments using an instrumented impact hammer and making a force comparison.

3. Results

3.1 Compliance Correction

During quasi-static, intermediate, and high-rate experiments, the compliance of the gripping system must be taken into account for accurate determination of strain measurements. ASTM C1557-03 (*7*) describes a method to account for system compliance. The system compliance must be determined experimentally for a given test machine, gripping system, and fiber type (*7*). The system compliance is determined by plotting apparent compliance (mm/N) versus l_0/A, as shown in figure 4. The cross-head displacement ΔL is measured from the system, and A is the cross-sectional area of the fiber based on the accurate measurement of diameter in the SEM. F is the breaking force and l_0 is the gage length. A gage length of zero represents the system compliance. The intercept of the linear fit is this system compliance (C_s). A typical apparent compliance curve is shown in figure 4; the value of C_s is 0.113 in the case shown in figure 4. Apparent compliance was calculated for each fiber type (unwoven, warp, weft) at each strain rate (low, intermediate, and high rate). The variability in the data at the longer gage lengths is due to variations in breaking force and/or fiber diameter.

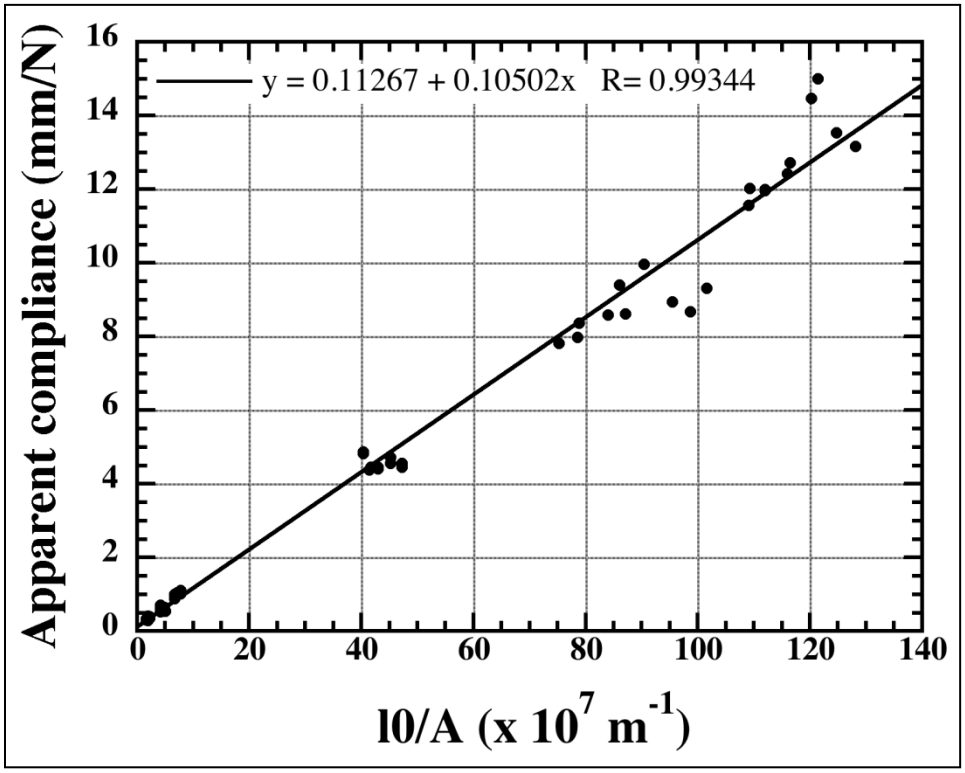

Figure 4. Typical apparent compliance curve. This particular data is from weft fibers tested at quasi-static rate.

The strain measurement is then corrected using the value of C_s determined by the linear fit in figure 4. The corrected strain is (*7*)

$$\varepsilon_{corrected} = \frac{\Delta L - C_s F}{l_0}. \quad (6)$$

Similarly, Young's modulus must also be corrected

$$E_{corrected} = \frac{l_0}{A(C_A - C_s)}, \quad (7)$$

where C_a is the apparent compliance in mm/N. The corrected strain behavior is shown in figure 5. The compliance correction lowers the failure strain at the shorter gage lengths more when compared to the longer gage lengths. The short gage length of 2 mm is especially affected by the correction; a reduction in failure strain of around 35% is shown in figure 5.

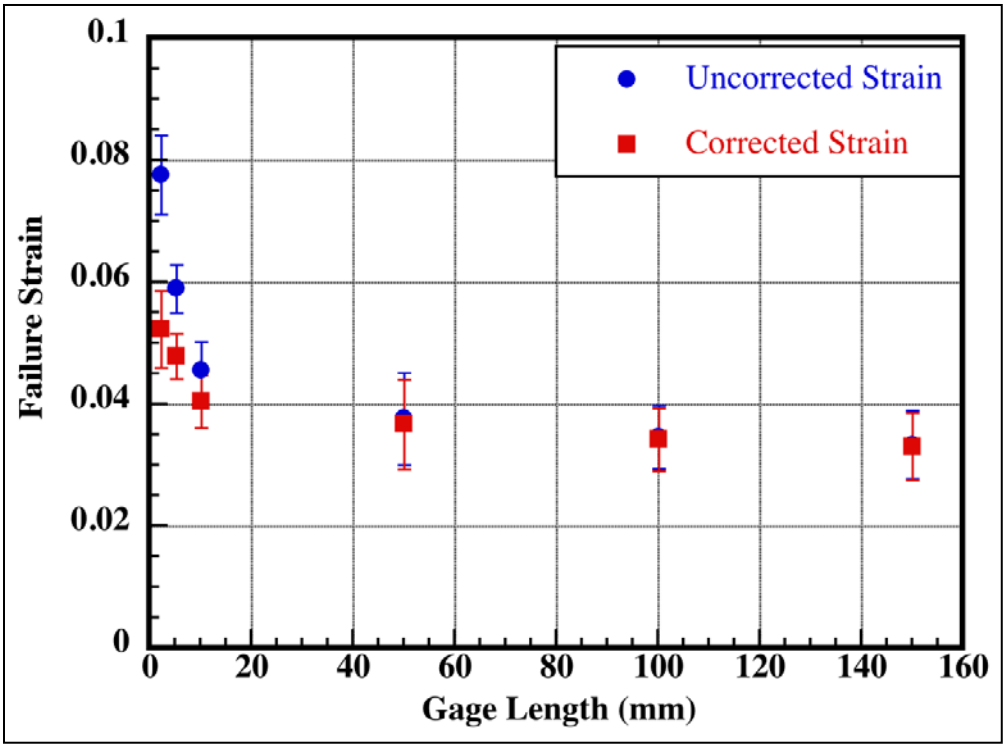

Figure 5. Compliance corrected strain measurements. This particular data is from weft fibers tested at quasi-static rate.

A correction to Young's modulus was made and is shown in figure 6. After applying equation 7 to the blue data points shown in figure 6 to account for the system compliance, the red data points give a more accurate representation of Young's modulus behavior of the fiber. Note that shorter gage lengths are more affected by Young's modulus correction than the longer gage lengths.

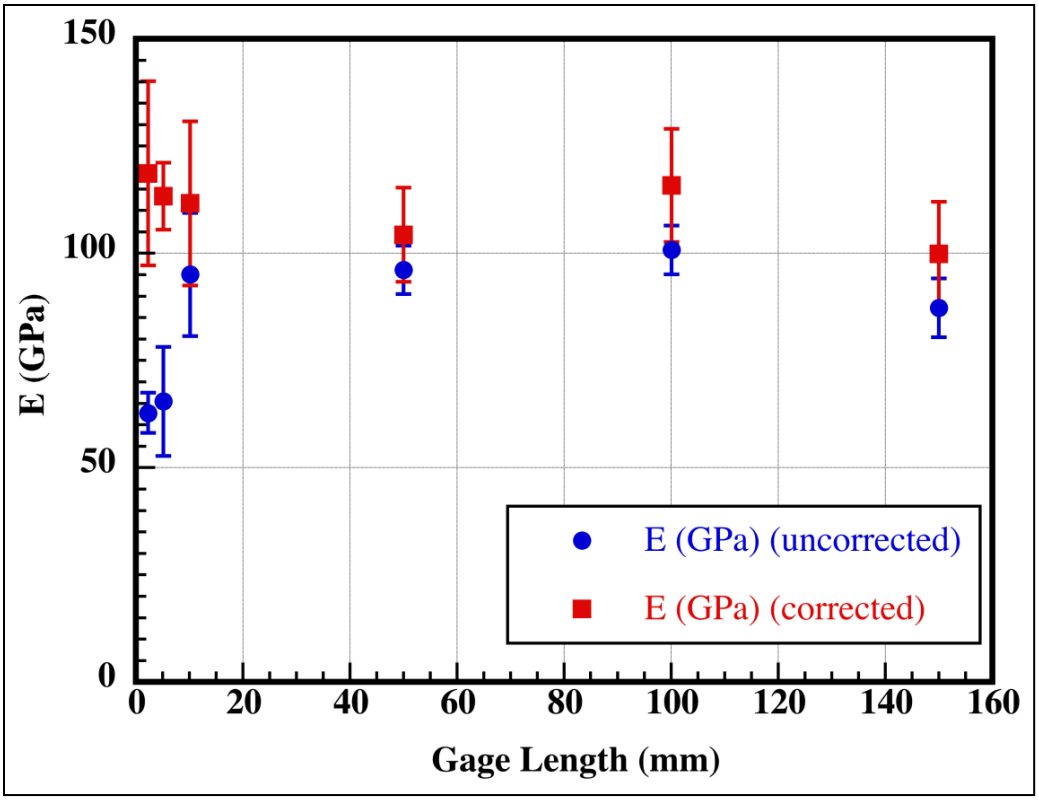

Figure 6. Typical Young's modulus corrected using equation 7 at multiple gage lengths. This particular data is from weft fibers tested at quasi-static rate.

The modulus of the fiber was also studied as a function of strain rate and is shown in figure 7. A table of this data is shown in the appendix. The unwoven and weft fibers showed a modest increase in stiffness with an increase in strain rate; the moduli increased approximately 65% with an increase in strain rate of 1200 s^{-1}. The modulus of the warp fibers increased about 27% from low to intermediate rate. The modulus for warp fibers at high rate could not be determined due to the wide scatter in the data.

Young's modulus results derived from only long gage length samples are shown in figure 8. A table of this data is shown in the appendix. Young's modulus values at gage lengths greater than 10 mm are taken to be the gage length independent of Young's modulus and are discussed in section 4. The strain rates here are limited to low and intermediate rates since long (approximately 10 mm +) samples cannot be tested at high-strain rates due the inability to reach the required dynamic equilibrium constraint during the experiment. Figure 8 shows that the unwoven fibers had the highest modulus at around 112.1 ± 1.89 GPa while the warp and weft fibers were 91.5 ± 6.22 GPa and 103.7 ± 4.26 GPa, respectively. These values are within the range noted by Lim et al. (*8*) for Kevlar 129. The warp fibers showed an 18% reduction in stiffness while the weft fibers showed a 7% drop in stiffness.

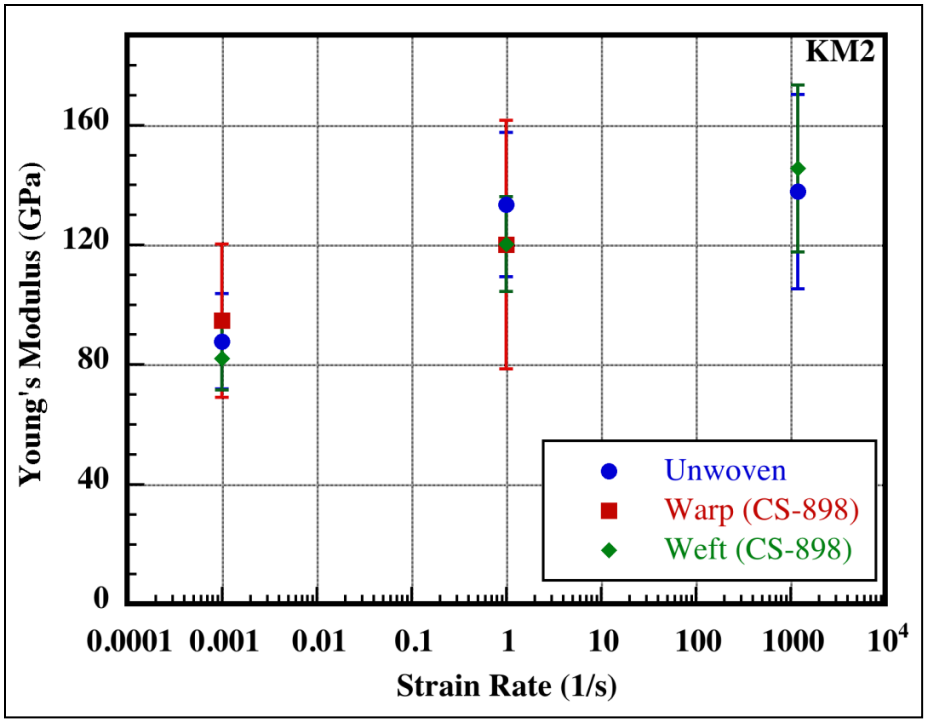

Figure 7. Tensile Young's modulus as a function of strain rate over short gage lengths. The values in this plot represent averages of the 2-, 5-, and 10-mm gage length fibers so comparisons can be made over the three strain rates.

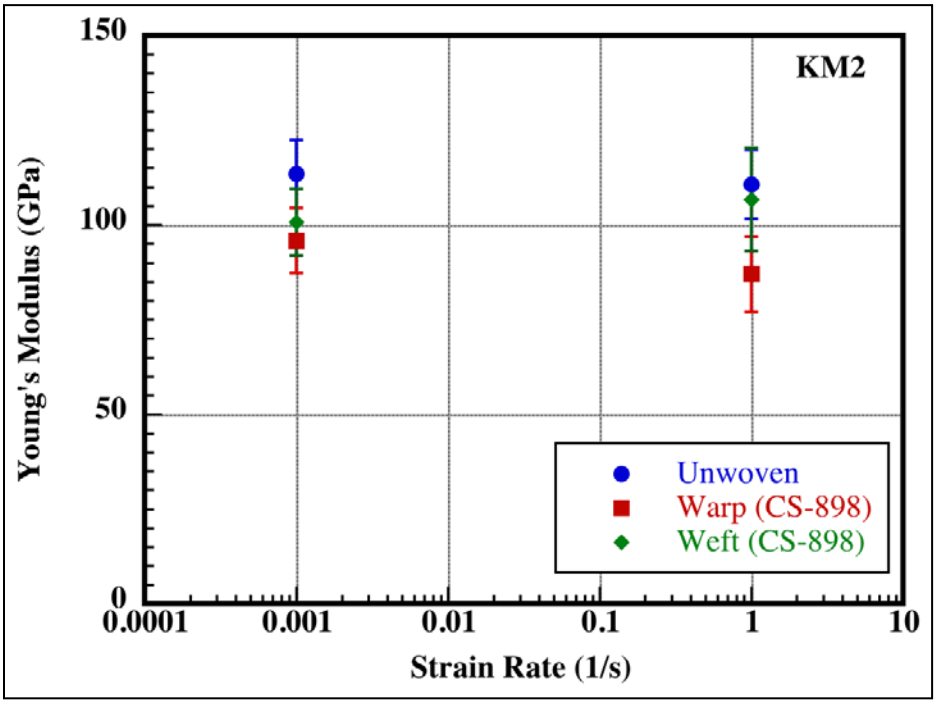

Figure 8. Young's modulus at low and intermediate rates of long gage length fibers. The values in this plot represent averages over the 50-, 100-, and 150-mm gage length fibers, which are taken to be gage length independent.

3.2 Weave Effects at Three Strain Rates

A typical raw data output from a high-rate experiment is shown in figure 9. Strain in the incident bar was recorded using semiconductor strain gages, while the transmitted signal was recorded using a piezoelectric force transducer. The relatively flat pulses were obtained through use of a thin copper pulse shaper.

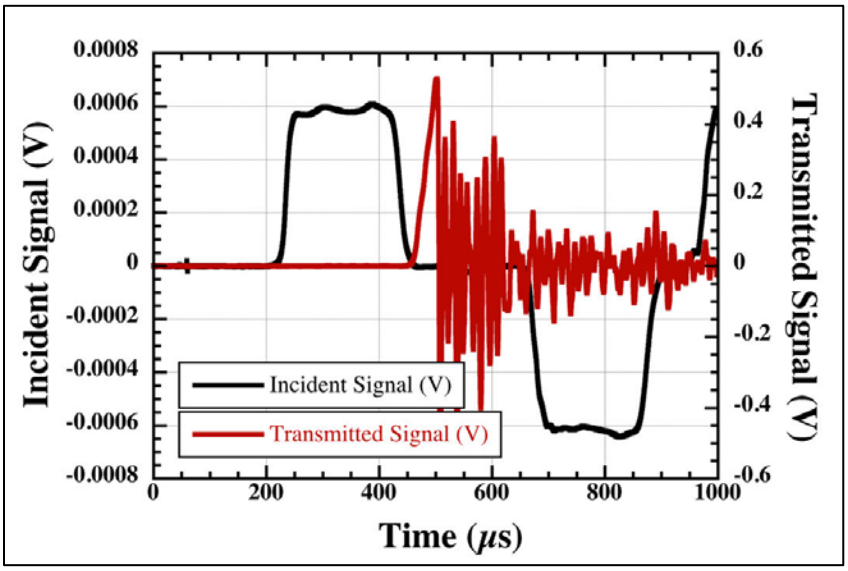

Figure 9. Raw data from a high-rate experiment.

A typical strain rate and stress history from a high-rate experiment on an unwoven Kevlar fiber is shown in figure 10. This experimental record shows that after a ramp time of around 60 μs the fiber reached a constant strain rate of about 1150 s^{-1} until failure occurred at 90 μs.

Results averaged over the 2-, 5-, and 10-mm gage lengths over the three strain rates are shown in figure 11. A table of the data from which this figure was created is shown in the appendix. At all strain rates the unwoven fibers were stronger than either the warp or weft fibers. Degradation in strength of the warp and weft fibers is also noted in figure 9. Fibers taken from the weft direction of the woven fabric were about 3%–8% weaker than the unwoven fibers. A larger difference was seen when comparing the unwoven fibers to the warp fibers. The warp fibers showed a minimum of 20% reduction in strength at intermediate and high rate and a 35% reduction in strength at low rate compared to unwoven fibers over the three short gage lengths examined. The warp and weft fibers also showed a higher amount of variability in failure strength evinced by larger scatter bands.

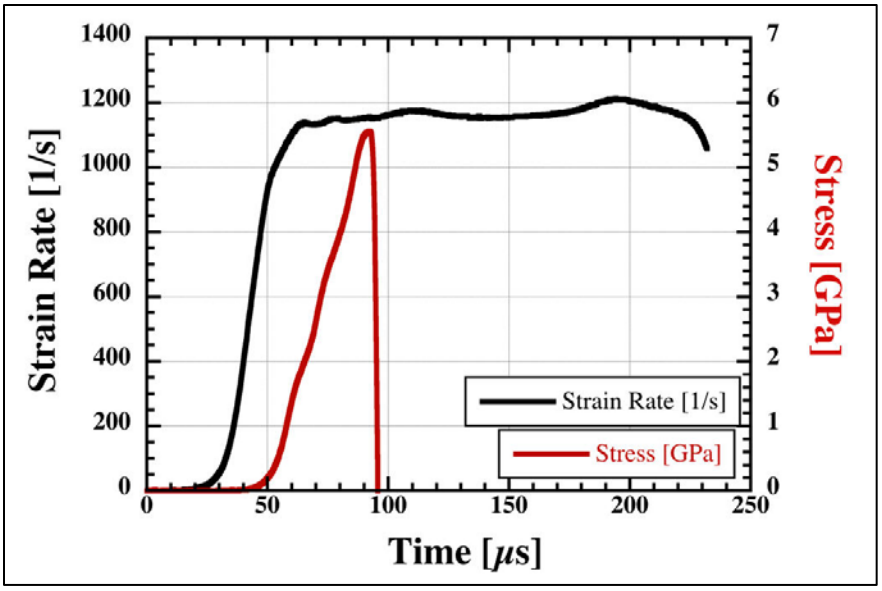

Figure 10. Strain rate and stress histories from a high-rate experiment on a single Kevlar KM2 fiber.

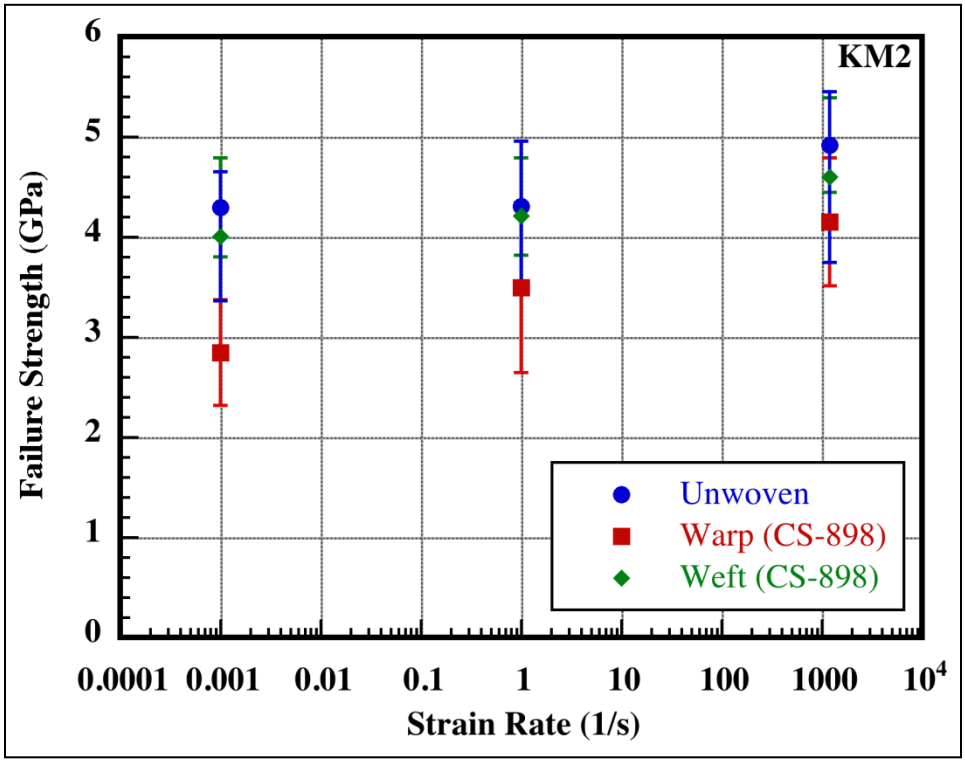

Figure 11. Tensile strength Kevlar KM2 single fibers as a function of strain rate.

3.3 Gage Length Effects and Damage Distribution

In an attempt to quantify defects inherent in the fiber over a given length, multiple gage lengths were examined. The effect of gage length at quasi-static and intermediate rates is shown in figures 12 and 13. A table of data from which these figures were created is shown in the appendix. For both low and intermediate strain rates the tensile strength decreased with increasing gage length for the all fiber types. In general the ultimate strength did not decrease a significant amount. Only once the length scale is reduced to 5 mm is there a reduction in apparent defects seen by an increase in strength.

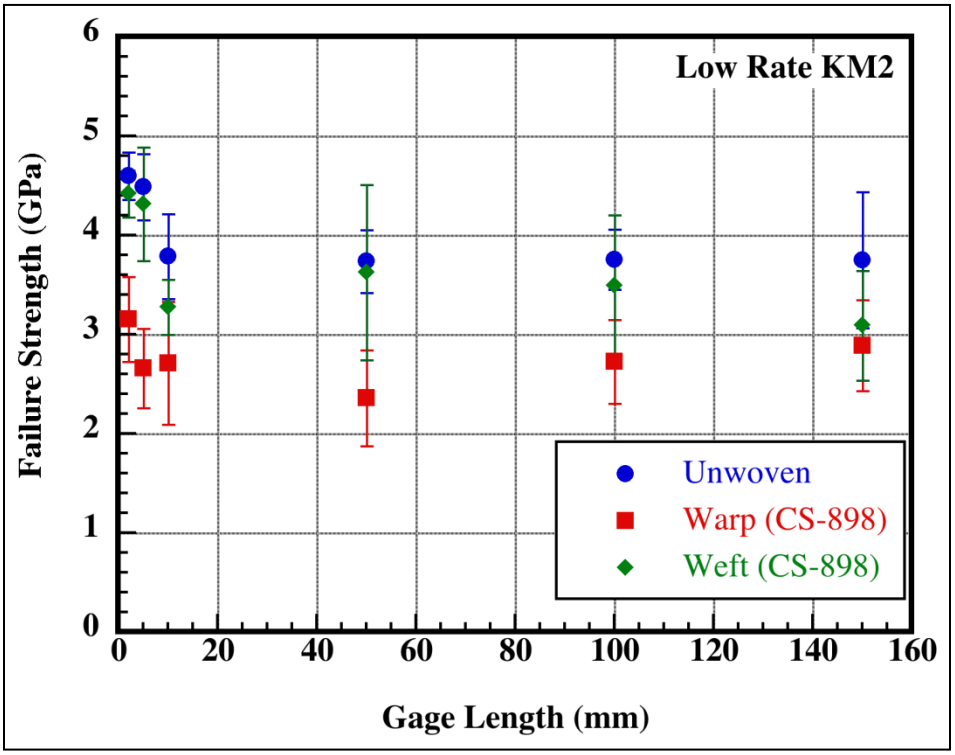

Figure 12. Variation of strength with respect to gage length at low rate showing the effect of defect distribution.

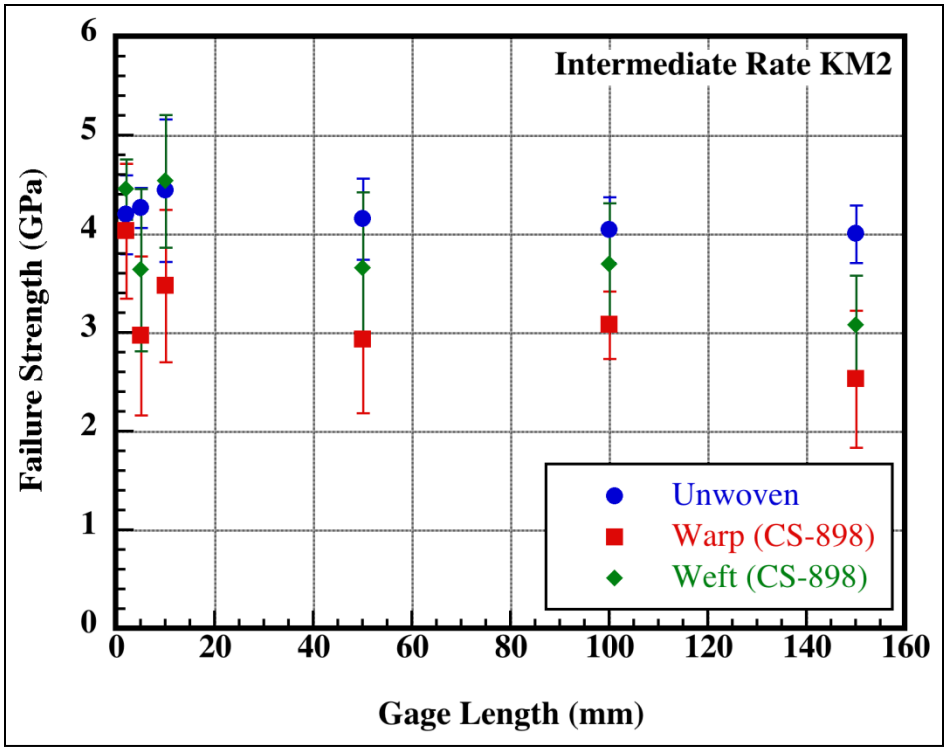

Figure 13. Gage length variation at intermediate rate showing the effect of defect distribution.

The gage length dependence at high-loading rate is shown in figure 14. A table of data from which these figures were created is shown in the appendix. Unwoven fibers showed a small increase in failure strength of 2% in the 2-mm gage length samples when compared to the 10-mm gage length samples. Warp and weft fibers showed different behavior. The strength of the warp fibers increased 17.5% in the 2-mm gage length compared to the 10-mm case. The strength of the weft fibers did not change significantly; a 4% decrease in strength was noted over the same range as the other fibers. The size of the scatter was large for the weft fibers compared to the unwoven fibers.

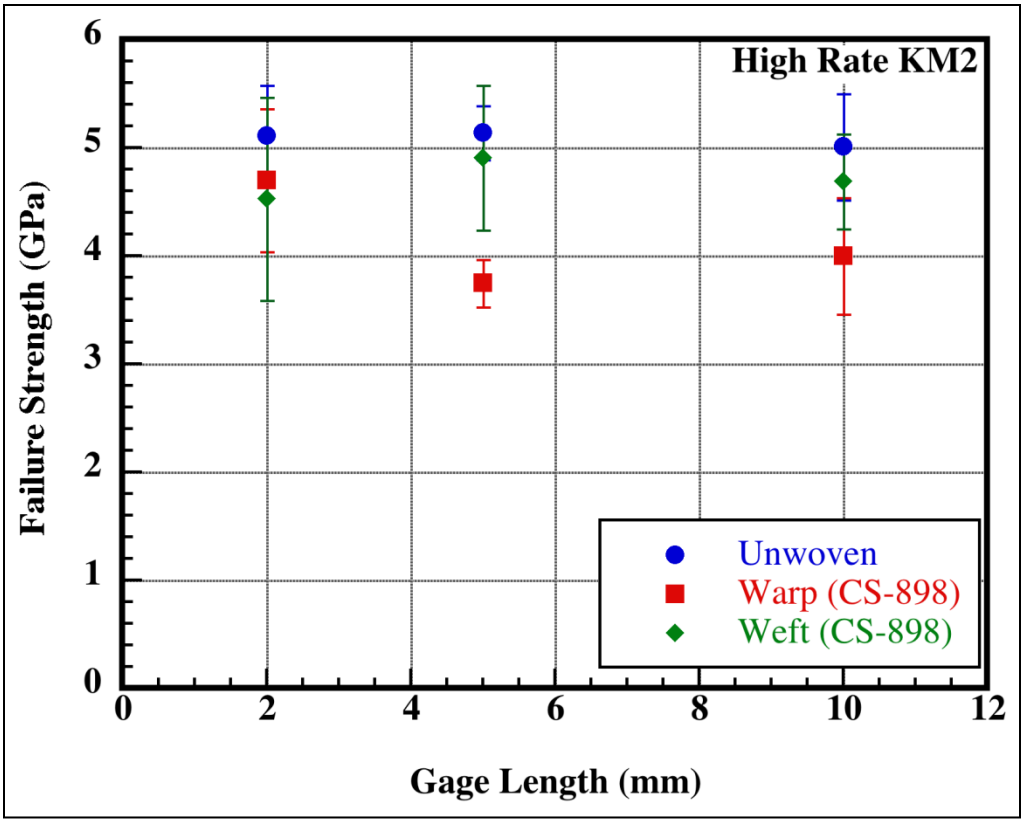

Figure 14. Gage length variation at high rate showing the effect of defect distribution.

4. Discussion

In general, Young's modulus of all three fiber types decreased with decreasing gage length. This decreasing modulus in respect to decreasing gage length was also noted by Lim et al. (*5*). The error between the corrected and uncorrected Young's modulus decreases past a gage length of approximately 10 mm. This may be due to the sensitivity of the system compliance, *Cs*. Small changes to the slope of the compliance curve have a greater affect on the corrected modulus and strain values. Lim et al. (*5*) did not conjecture why the modulus would be lower for the shorter fibers but instead stated that the error between uncorrected and corrected values decreased past a gage length of 10 mm, and took the modulus at longer gage lengths to be gage length independent. Due to the sensitivity of Young's modulus at short gage lengths, the results summarized in figure 7 at three different strain rates do not represent the gage length independent Young's modulus. However, averaging the modulus over the 2-, 5-, and 10-mm gage lengths for the three strain rates allows for a qualitative comparison to investigate the rate dependence on modulus. The behavior shown in figure 7 suggests that Kevlar increases in stiffness with loading rate.

Considering the gage length independent modulus behavior shown in figure 8, fibers from the warp and weft directions of the hydrophobic fabric had lower stiffness compared to the unwoven fibers. Weft fibers were generally less stiff than the warp fibers at both low and intermediate rate. The reduction in stiffness of the warp fibers may be attributed to the fibers being held in tension during weaving, the crimping process, the scouring process, or application of the fluoropolymer. Studies of the single fiber behavior of greige and scoured fabric would help delineate this finding.

The Kevlar fibers in this study showed an increase in strength with increasing strain rate. Qualitatively, the data shown in figure 11 are consistent with the rate dependence seen by other authors (*5*, *6*, *8*, *10*) for aramid fibers. Cheng et al. (*3*) did not see a marked increase in strength with increasing strain rate; Cheng et al. (*3*) found that the strength of unwoven Kevlar KM2 increased from 3.88 ± 0.40 GPa at quasi-static rate, while the high-rate failure strength was 4.04 ± 0.38 GPa. In this study, the failure of strength of unwoven KM2 increased from 4.30 ± 0.49 GPa to 5.1 ± 0.41 GPa from quasi-static to high rate.

The magnitude of the decrease in strength of warp and weft fibers is similar to that seen by Nilakantan et al. (*9*) from experiments on yarns. Nilakantan et al. (*9*) saw a decrease in strength for warp yarns of about 15%–20% and 30% for greige and scoured yarns, respectively. Weft yarns were 6%–9% weaker for greige and 10%–16% weaker for scoured. The ranges given in the work by Nilakantan et al. (*9*) depended on the gage length and the probability of failure calculated using a three-parameter Weibull method. The differences in the strength of the woven single fibers in this study compared to the unwoven fibers could be attributable to the crimping process, frictional sliding of the weft fibers against the warp fibers during weaving, the warp fibers being held in tension during weaving, or from the finishing process including scouring or application of the hydrophobic finish. Other factors could be present, but due to the proprietary nature of the fiber weaving and processing process additional fiber degradation factors are hard to track.

Fibers taken from the warp and weft directions were 20%–35% and 3%–8% weaker than unwoven fibers over the range of strain rates. These ranges are similar to the ranges found by Nilakantan et al. (*9*) on yarn experiments at quasi-static rate; however, single fiber and yarn experimental results are not directly comparable due to possible interactions of the single fibers within the yarn during breaking or failure. Attributing the measured reduction in strength of the warp and weft single fibers to any single step of the weaving and finishing process is difficult since single fiber experiments were not conducted on woven yarns taken from intermediate steps of the weaving process, from greige (woven, unscoured, untreated), to scoured (woven, scoured, untreated), to hydrophobic finish (woven, scoured, treated). Only a full experimental investigation of single fiber response including the greige and scoured fabric would show the effects of the different handling, weaving, scouring, and surface treatment on the single fiber response.

The investigation of gage length and hence defect distribution indicates that defects are evenly distributed along the fiber once the gage length is longer than 10 mm. Similar behavior was seen in the single fiber gage length study by Lim et al. (*5, 8*). Nilakantan et al. (*9*) also saw length-scale effects while experimenting with yarns at quasi-static rates. When experiments were conducted at high-strain rate, the Kevlar fiber showed a weak increase in failure strength. The increase in strength of the 2-mm gage length to the 10-mm gage length was only about 2% for the unwoven case. This result agrees with experiments on Kevlar 129 fibers by Lim et al. (*6*) who noted only a 4% increase in failure strength between the 2- and 10-mm gage length samples.

5. Summary

Single fiber experiments were conducted on fibers extracted from the two weaving directions of plain woven, hydrophobically treated Kevlar KM2 and compared to fibers extracted from an unwoven yarn to elucidate any damage due to the weaving and finishing process to the single fibers. The strain rate dependence of the three fiber types was studied over a strain rate range of 0.001–1200/s using a Bose Electroforce test bench and a fiber-SHTB equipped with a noncontact laser strain measuring system. The gage length dependence of the fiber was also studied over the three strain rates to discover the distribution of defects along the fiber.

An analysis of the tensile Young's modulus was also carried out, accounting for variation in the compliance of the testing systems. After correcting for system compliance, the data show that the modulus for short gage length unwoven and weft fibers increased 65% over the range of strain rates. Modulus obtained from long gage length samples, taken to be the gage length independent modulus, showed an 18% drop for warp fibers while the weft fibers were 7% less stiff compared to unwoven fibers. Attributing this reduction in stiffness to a particular step of the weaving or finishing process is difficult since the fibers studied had been woven, scoured, and hydrophobically treated.

All fiber types showed a small increase in strength as the strain rate increased from 0.001 to 1200/s despite any effects of weaving or finishing. In addition to the strain rate effect, changes in strength due to weaving were also present. The warp fibers were a minimum of 20% weaker than the unwoven fibers at all strain rates, and were 35% weaker at quasi-static strain rate. Weft fibers were 3%–8% weaker over the range of strain rates. The reduction in strength of the warp fibers could be attributed to the weaving and finishing process, however the hydrophobically treated fibers used in this study were scoured in a separate step of the finishing process; hence, it is difficult to determine which step of the finishing process caused the degradation in strength. Further single fiber studies including fibers originating from greige and scoured fabric are needed to delineate these findings.

The gage length dependence from which defect distribution can be inferred showed that at shorter gage lengths the fiber strength increased, probably due to less defects present in the fiber at shorter gage lengths. This gage length dependence was consistent with similar experimental investigations on single fibers.

6. References

1. *Technical Fabrics Handbook*; Hexcel Corporation: Stamford, CT, December 2010, 64–65.
2. DeTeresa, S. J.; Allen, S. R.; Farris, R. J.; Porter. R. S. Compressive and Torsional Behavior of Kevlar 49 fibre. *Journal of Materials Science* **1984**, *19*, 57–72.
3. Cheng, M.; Chen, W.; Weerasooriya, T. Mechanical Properties of Kevlar KM2 Single Fiber. *Journal of Engineering Materials and Technology* **2005**, *127*, 197–203.
4. Cheng, M.; Chen, W.; Weerasooriya, T. Experimental Investigation of the Transverse Mechanical Properties of a Single Kevlar KM2 Fiber. *Int. Journal of Solids and Structures* **2004**, *41*, 6251–6232.
5. Lim, J.; Zheng, J. Q.; Masters, K.; Chen, W. W. Mechanical Behavior of A265 Single Fibers. *Journal of Materials Science* **2010**, *45*, 652–661.
6. Lim, J.; Chen, W. W.; Zheng, J. Q. Dynamic Small Strain Measurements of Kevlar 129 Single Fibers With a Miniaturized Tension Kolsky Bar. *Polymer Testing* **2010**, *29*, 701:705.
7. ASTM-C-1557-03. Standard Test Method for Tensile Strength and Young's Modulus of Fibers. *Annu. Book ASTM Stand* **2008**.
8. Lim, J.; Zheng, J. Q.; Masters, K.; Chen, W. W. Effects of Gage Length Loading Rates, and Damage on the Strength of PPTA Fibers. *International Journal of Impact Engineering* **2011**, *38*, 219–227.
9. Nilakantan, G.; Obaid, A. A.; Keefe, M.; Gillespie, J. W. Experimental Evaluation and Statistical Characterization of the Strength and Strain Energy Density Distribution of Kevlar KM2 Yarns: Exploring Length-Scale and Weaving Effects. *Journal of Composite Materials* **2011**, *45* (17) 1749–1769.
10. Sanborn, B.; Racine, N.; Weerasooriya, T. *The Effect of Weaving on the Strength of Kevlar KM2 Single Fibers at Different Loading Rates*; ARL-TR-6280; U.S. Army Research Laboratory: Aberdeen Proving Ground, MD, December 2012.

Appendix

Table A-1. Rate dependence on Young's modulus. These values were found by averaging Young's modulus of the 2-, 5-, and 10-mm gage length samples.

Strain Rate	Unwoven Young's Modulus (GPa)	Warp (CS-898) Young's Modulus (GPa)	Weft (CS-898) Young's Modulus (GPa)
0.001	87.74 ± 15.96	94.63 ± 25.58	82.00 ± 10.54
1	133.40 ± 24.12	120.03 ± 41.53	120.17 ± 15.87
1200	137.78 ± 32.45	—	145.52 ± 27.86

Table A-2. Rate dependence on Young's modulus. These values were found by averaging Young's modulus of the 50-, 100-, and 150-mm gage length samples

Strain Rate	Unwoven Young's Modulus (GPa)	Warp (CS-898) Young's Modulus (GPa)	Weft (CS-898) Young's Modulus (GPa)
0.001	113.43 ± 8.98	95.92 ± 8.58	100.72 ± 8.70
1	110.76 ± 9.19	87.12 ± 9.94	106.74 ± 13.60

Table A-3. Failure strength of fibers tested at quasi-static rate.

Gage Length (mm)	Unwoven Strength (GPa)	Warp (CS-898) Strength (GPa)	Weft (CS-898) Strength (GPa)
2	4.60 ± 0.24	3.16 ± 0.43	4.42 ± 0.23
5	4.49 ± 0.33	2.66 ± 0.40	4.32 ± 0.57
10	3.79 ± 0.43	2.71 ± 0.62	3.28 ± 0.28
50	3.74 ± 0.32	2.36 ± 0.48	3.63 ± 0.88
100	3.76 ± 0.30	2.73 ± 0.42	3.49 ± 0.71
150	3.75 ± 0.69	2.89 ± 0.46	3.09 ± 0.55

Table A-4. Failure strength of fibers tested at intermediate rate.

Gage Length (mm)	Unwoven Strength (GPa)	Warp (CS-898) Strength (GPa)	Weft (CS-898) Strength (GPa)
2	4.20 ± 0.40	4.03 ± 0.68	4.46 ± 0.30
5	4.27 ± 0.20	2.98 ± 0.81	3.64 ± 0.82
10	4.44 ± 0.72	3.48 ± 0.77	4.54 ± 0.67
50	4.16 ± 0.41	2.93 ± 0.74	3.66 ± 0.77
100	4.04 ± 0.33	3.08 ± 0.34	3.69 ± 0.62
150	4.00 ± 0.29	2.54 ± 0.69	3.08 ± 0.51

Table A-5. Failure strength of fibers tested at high rate.

Gage Length (mm)	Unwoven Strength (GPa)	Warp (CS-898) Strength (GPa)	Weft (CS-898) Strength (GPa)
2	5.11 ± 0.47	4.7 ± 0.66	4.53 ± 0.94
5	5.14 ± 0.25	3.75 ± 0.22	4.91 ± 0.67
10	5.01 ± 0.49	4.00 ± 0.54	4.69 ± 0.44

Table A-6. Failure strength of fibers tested at multiple strain rates. These values are averages over the 2-, 5-, and 10-mm gage lengths.

Strain Rate (1/s)	Unwoven Strength (GPa)	Warp (CS-898) Strength (GPa)	Weft (CS-898) Strength (GPa)
0.001	4.30 ± 0.49	2.84 ± 0.53	4.01 ± 0.65
1	4.30 ± 0.49	3.50 ± 0.85	4.21 ± 0.74
1200	5.10 ± 0.41	4.15 ± 0.64	4.71 ± 0.71

NO. OF COPIES	ORGANIZATION
1 (PDF)	DEFENSE TECHNICAL INFORMATION CTR DTIC OCA
1 (PDF)	DIRECTOR US ARMY RESEARCH LAB RDRL CIO LL
1 (PDF)	GOVT PRINTG OFC A MALHOTRA
1 (PDF)	US ARMY ABERDEEN TEST CTR TEDT AT SLB A FOURNIER
1 (PDF)	PURDUE UNIV DEPT OF AERONAUTICS AND ASTRONAUTICS WAYNE CHEN
1 (PDF)	UNIV OF NORTH TEXAS DEPT OF MECHL & ENERGY ENGRNG XU NIE
2 (PDF)	MASSACHUSETTS INST OF TECHLGY INST FOR SOLDIER NANOTECHNOLOGIES R RADOVITZKY S SOCRATE
1 (PDF)	HUMAN SYSTEMS DEPT NVL AIR WARFARE CTR AIRCRAFT DIV B SHENDER
2 (PDF)	DEPT OF MECHL ENGRNG THE JOHNS HOPKINS UNIV LATROBE 122 K T RAMESH V NGUYEN
1 (PDF)	UNIV OF TEXAS AUSTIN AEROSPACE ENGRNG AND ENGRNG MECHS K RAVI-CHANDAR
1 (PDF)	NVL SURFACE WARFARE CTR CODE 664 P DUDT
2 (PDF)	JTAPIC PROG OFC US ARMY MEDICAL RSRCH AND MTRL CMND MRMC RTB J USCILOWICZ F LEBEDA
1 (PDF)	TARDEC RDTA RS R SCHERER
1 (PDF)	NATICK SOLDIER RSRCH DEV AND ENGRNG CTR NSRDEC AMSRD NSC WS TB M G CARBONI
6 (PDF)	NATICK SOLDIER RSRCH DEV AND ENGRNG CTR NSRDEC RDNS D M CODEGA RDNS WPW P R DILALLA RNDS TSM M STATKUS RDNS WSD B J WARD P CUNNIFF M MAFFEO
2 (PDF)	SOUTHWEST RSRCH INST MECHL AND MTRLS ENGRG DIV MTRLS ENGRG DEPT D NICOLELLA W FRANCIS
1 (PDF)	SANDIA NATL LABS PO BOX 969 MS 9404 B SONG
1 (PDF)	THE UNIV OF UTAH K L MONSON
1 (PDF)	COLUMBIA UNIV 351 ENGINEERING TERRACE B MORRISON
1 (PDF)	APPLIED RSRCH ASSOC INC SOUTHWEST DIV C E NEEDHAM

NO. OF COPIES ORGANIZATION

2 (PDF) CTR FOR INJURY BIOMECHANICS
WAKE FOREST UNIV
J STITZEL
F S GAYZIK

1 (PDF) US INFANTRY CTR
MTRLS LOG NCO SCI TECHNLGY ADVISOR
SOLDIER DIV
S VAKERICS

3 (PDF) NATL GROUND INTLLGNC CTR
D EPPERLY
T SHAVER
T WATERBURY

2 (PDF) PROG EXECUTIVE OFC SOLDIER
K MASTERS
J ZHENG

2 (PDF) SOUTHWEST RSRCH INST
T HOLMQUIST
G JOHNSON

1 (PDF) AIR FORCE RSRCH LAB
AFRL RWMW
B MARTIN

4 (PDF) DRDC VALCARTIER
K WILLIAMS
A BOUAMOUL
L MARTINEAU
D NANDLALL

1 (PDF) DRDC TORONTO
C BURRELL

1 (PDF) HUMAN PROTECTION AND PERFORM DIV
DEFENCE SCI AND TECHLGY ORGN
DEPT OF DEFENCE
T RADTKE

1 (PDF) DEFENCE SCI AND TECHLGY ORGN
S WECKERT

U.S. ARMY RESEARCH LABORATORY

105 (PDF) DIR USARL
RDRL CIH C
P CHUNG
RDRL HRS C
W HAIRSTON
B LANCE
K MCDOWELL
K OIE
J VETTEL
RDRL ROE M
D STEPP
RDRL ROE N
L RUSSELL
RDRL DP
R COATES
R SPINK
RDRL SLB A
B WARD
RDRL SLB W
A BREUER
N EBERIUS
P GILLICH
C KENNEDY
A KULAGA
W MERMAGEN
K RAFAELS
L ROACH
RDRL WM
P BAKER
B FORCH
S KARNA
J MCCAULEY
P PLOSTINS
RDRL WML
M ZOLTOSKI
RDRL WML A
W OBERLE
RDRL WML F
G BROWN
RDRL WML G
J SOUTH
RDRL WML H
T EHLERS
M FERMEN-COKER
L MAGNESS
C MEYER
J NEWILL
D SCHEFFLER
S SCHRAML
RDRL WMM
J BEATTY
B DOWDING
RDRL WMM A
R EMERSON
D O'BRIEN
E WETZEL
RDRL WMM B
R CARTER
B CHEESEMAN
G GAZONAS

NO. OF COPIES ORGANIZATION

B LOVE
P MOY
C RANDOW
C YEN
RDRL WMM C
A BUJANDA
R JENSEN
J LA SCALA
J YIM
RDRL WMM D
E CHIN
S WALSH
W ZIEGLER
RDRL WMM E
G GILDE
J LASALVIA
P PATEL
J SINGH
J SWAB
RDRL WMM F
S GRENDAHL
E KLIER
L KECSKES
RDRL WMM G
J LENHART
R MROZEK
A RAWLETT
K STRAWHECKER
RDRL WMP
S SCHOENFELD
RDRL WMP B
A DAGRO
A DWIVEDI
A GUNNARSSON
C HOPPEL
M LYNCH
D POWELL
B SANBORN
S SATAPATHY
M SCHEIDLER
T WEERASOORIYA
RDRL WMP C
R BECKER
S BILYK
T BJERKE
J BRADLEY
D CASEM
J CLAYTON
D DANDEKAR
M GREENFIELD
B LEAVY

NO. OF COPIES ORGANIZATION

C MEREDITH
M RAFTENBERG
C WILLIAMS
RDRL WMP D
R DONEY
D KLEPONIS
J RUNYEON
B SCHUSTER
B SCOTT
B VONK
RDRL WMP E
S BARTUS
M BURKINS
D HACKBARTH
RDRL WMP F
A FRYDMAN
E FIORAVANTE
N GNIAZDOWSKI
R GUPTA
R KARGUS
RDRL WMP G
N ELDREDGE
RDRL WMS
M VANLANDINGHAM